

Synthesis of TiO₂ porous thin films by polyethylene glycol templating and chemistry of the process

S. J. Bu, Z. G. Jin*, X. X. Liu, L. R. Yang, Z. J. Cheng

Key Laboratory for Advanced Ceramics and Machining Technology of Ministry of Education, School of Materials, Tianjin University, Tianjin 300072, China

Received 11 November 2003; accepted 20 December 2003

Available online 20 July 2004

Abstract

Titanium dioxide porous films have been deposited on glass slides by sol–gel technology. Tetrabutylorthotitanate and polyethylene glycol were used as a precursor and template, respectively. The chemical mechanism is discussed in relation to the sol–gel transition, which provides a possible theoretic explanation to the formation of TiO₂ porous films. The morphology of porous TiO₂ thin films strongly depends on the amount of water, the types of solvents and complexing agents, and the concentration and molecular weight of the template. It was shown that the diameter of pores is tunable in the range of 10–500 nm and the maximum of BET specific area of the films is 72 m²/g.

© 2004 Elsevier Ltd. All rights reserved.

Keywords: TiO₂; Porous thin films; Templating; Polyethylene glycol

1. Introduction

Since the pioneering work by Fujishima et al.¹, titanium dioxide (TiO₂) has been one of the most attractive photoelectrochemical and photovoltaic materials during the last decades due to its scientific and technological importance. And TiO₂ porous thin films with a relatively large surface area are desired for many applications, such as photocatalysts,² transparent conductors,³ dielectrics,⁴ electrochromic films,⁵ and “self-cleaning” coatings on windows and tiles.⁶ The TiO₂-dye composite material was reported to harvest a high proportion of the solar energy, and it is expected to serve for manufacturing low-cost solar cells.^{7,8}

In recent years, a great interest in nanocrystalline TiO₂ porous films has been growing. Many papers have been published on the preparation of porous titania films using the sol–gel method,⁹ direct deposition from aqueous solutions,¹⁰ sputtering technology,¹¹ ultrasonic spray pyrolysis,¹² and hydrothermal crystallization.¹³ The sol–gel method of preparing TiO₂ films on the substrates has many advantages over other methods such as chemical vapor deposition (CVD),¹⁴ plasma spraying,¹⁵ anodization,¹⁶ and thermal oxidation of Ti metal¹⁷ mainly because of the following: (1) no special apparatuses are required; (2) uniform

multicomponent films can easily be formed if a homogeneous solution is available; (3) phase structure of films can be controlled, in this case TiO₂ (anatase) may be obtained; (4) the resultant films may be characterized by a porous structure of a gel with a large specific area characteristic. Recently, TiO₂ thin films of high specific area were also obtained from a TiO₂ sol prepared by hydrothermal treatment of peroxotitanic acid sol¹⁸ or an alkoxide-derived TiO₂ gel.¹⁹

In this work, we present results of investigations on processing and structural characteristics of TiO₂ porous thin films deposited on glass substrates through the sol–gel technology using polyethylene glycol (PEG) as a template. The influences of concentration and type of PEG templates, the amount of water added, the complexing agents and solvents were involved in this study because the morphologies of porous films are sensitive to them.

2. Experimental

2.1. Chemicals

For the preparation of TiO₂ sol, the following materials were used: polyethylene glycol ($M_{av} = 1000$ or 2000, H(OCH₂CH₂)_nOH; PEG), tetrabutylorthotitanate ($M = 340.35$, Ti(OC₄H₉)₄; Ti(OBu)₄), ethanolamine ($M = 61.08$, NH₂CH₂CH₂OH; EA), diethanolamine ($M = 105.14$,

* Corresponding author.

E-mail address: zhgj@tju.edu.cn (Z.G. Jin).

$\text{NH}(\text{CH}_2\text{CH}_2\text{OH})_2$; DEA), triethanolamine ($M = 149.19$, $\text{N}(\text{CH}_2\text{CH}_2\text{OH})_3$; TEA), acetylacetone ($M = 100.12$, $\text{CH}_3(\text{CO})\text{CH}_2(\text{CO})\text{CH}_3$; ACAC), glacial acetic acid ($M = 60.05$, CH_3COOH ; HAC), citrate acid ($M = 210.14$, $\text{C}_6\text{H}_8\text{O}_7 \cdot \text{H}_2\text{O}$; H₃L), ethanol ($M = 46.07$, $\text{CH}_3\text{CH}_2\text{OH}$; EtOH), and *n*-butanol ($M = 74.12$, $\text{CH}_3(\text{CH}_2)_2\text{CH}_2\text{OH}$).

2.2. Synthesis

TiO_2 porous films were prepared at room temperature in the following way: 8.68 ml of $\text{Ti}(\text{OBu})_4$ was dissolved in the mixture solution of 35 ml of EtOH/0.05 mol complexing agent. After magnetic stirring for 2 h, the obtained solution was hydrolyzed by the addition of a mixture of water and EtOH drop-wise under stirring for another 2 h. Then, various types and amounts of PEG were added into the TiO_2 sol, which was deposited on slide glasses by dip-coating with the withdrawing speed about 5–6 cm/min. The deposited films were aged at 100°C , and calcined at 550°C for 1 h in air to remove the organic template.

To investigate the effects of processing parameters on the porous texture of TiO_2 thin films, the following were adjusted in preparing sol: the molar ratio of water to $\text{Ti}(\text{OBu})_4$ was 1–3; the molecular weight of PEG was 1000 or 2000 and its adding amount was 0–4.0 g in 100 ml sol; the complexing agents were EA, DEA, TEA, ACAC, HAC, or H₃L; the solvent was EtOH or *n*-butanol. In all cases, while one parameter was changed, the others were held constant.

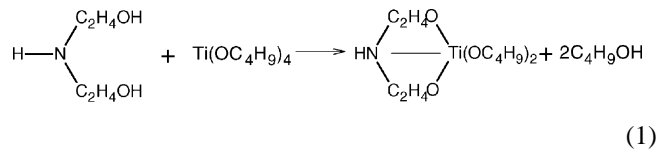
2.3. Characterization

Scanning electron microscope (SEM) images were taken on a PHILIPS XL-30 environment scanning electron micro-analyzer. IR spectra were recorded on BIO-RAD FTS3000 IR spectrometer. N_2 adsorption measurement was performed on a Quanta-chrome Nova 2000 specific area instruments.

3. Results and discussion

3.1. Chemistry of the sol–gel process

Chemical changes in sol–gel process can be deduced by analyzing FT-IR spectra of the specimens, depicted in Fig. 1. Firstly, It can be seen in traces 1 and 3 that the intensity of the N–H stretching vibration (3312 cm^{-1}) decreased and the C–N stretching vibration has a red-shift from 1129 to 1090 cm^{-1} , indicating that DEA has complexed with $\text{Ti}(\text{OBu})_4$. The complexing reactions taking place are presumed as follows:



The above reactions can restrain the hydrolysis and condensation of $\text{Ti}(\text{OBu})_4$ precursor, as a result of the increment

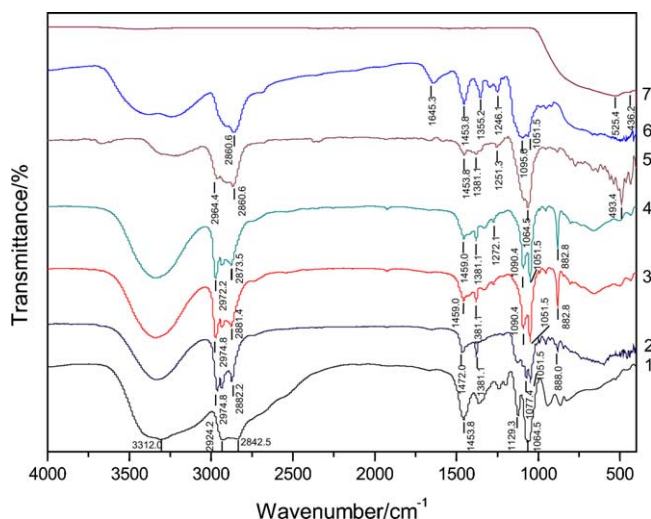
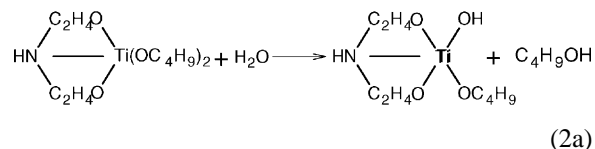


Fig. 1. IR spectra of titanium sol–gel process: (1) DEA, (2) $\text{Ti}(\text{OC}_4\text{H}_9)_4 + \text{C}_2\text{H}_5\text{OH}$, (3) $\text{Ti}(\text{OC}_4\text{H}_9)_4 + \text{C}_2\text{H}_5\text{OH} + \text{DEA}$, (4) $\text{Ti}(\text{OC}_4\text{H}_9)_4 + \text{C}_2\text{H}_5\text{OH} + \text{DEA} + \text{H}_2\text{O}$, (5) titanium colloid, (6) titanium xerogel, and (7) TiO_2 powders.

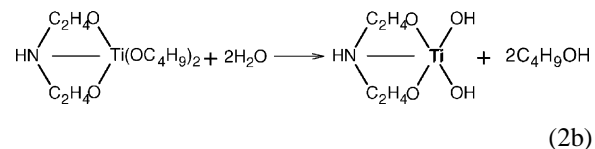
of the coordination number of Ti atom and the space steric hindrance.

For the hydrolysis and polycondensation reactions of $\text{Ti}(\text{OBu})_4$ precursor, the process can be written as below:

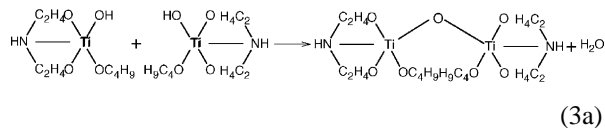
1. Hydrolysis



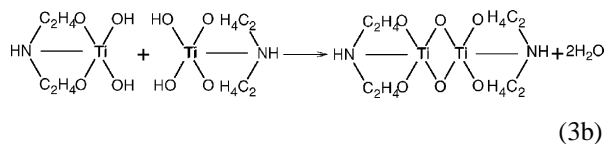
or



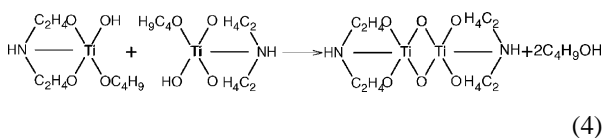
2. Dehydration polycondensation



or



3. Debutanation polycondensation



If the reactions above proceed, the Ti–O–C chemical bonding will be destroyed and weakened. In Fig. 1, it has been observed from curves 2–6 that the characteristic peak of Ti–O–C (2880 cm^{-1}) gradually shifted towards lower frequency, meanwhile decreasing in the intensity. This result can be good evidence that supports our assumption about the hydrolysis of $\text{Ti}(\text{OBU})_4$ and polycondensation of the hydrolysis products, shown in formulas.^{2–4}

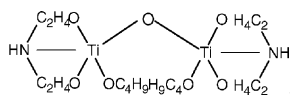
Furthermore, after PEG was added into the solution, the absorption peak from $-\text{O}-\text{C}_4\text{H}_9$ (880 cm^{-1}) disappeared. This implies that some polycondensations have occurred between PEG and the complex products, generating $\text{C}_4\text{H}_9\text{OH}$ as formula.⁵ Where PEG in the obtained inorganic–organic network configuration plays a role as the structure-directing agent, leading to the original morphology of TiO_2 porous films.

Bands at 1050 cm^{-1} belonging to the C–OH stretching vibration are observed in both of sol and xerogel IR spectra, which is attributed to the existence of alcohol. However, the intensity of xerogel weakened greatly and the peak characteristic for EtOH (800 cm^{-1}) disappeared in xerogel, proving that during gelating ethanol is released. The appearance of band at 1645 cm^{-1} shows the presence of hydrone in xerogel. For the TiO_2 powders after calcined at 550°C , the IR spectra mainly consists of two peaks at about 500 and 400 cm^{-1} , which are assigned to the absorption of anatase and rutile, while the organic substance has been removed completely.

3.2. Processing and porous texture

3.2.1. Effect of water to $\text{Ti}(\text{OBU})_4$ ratio

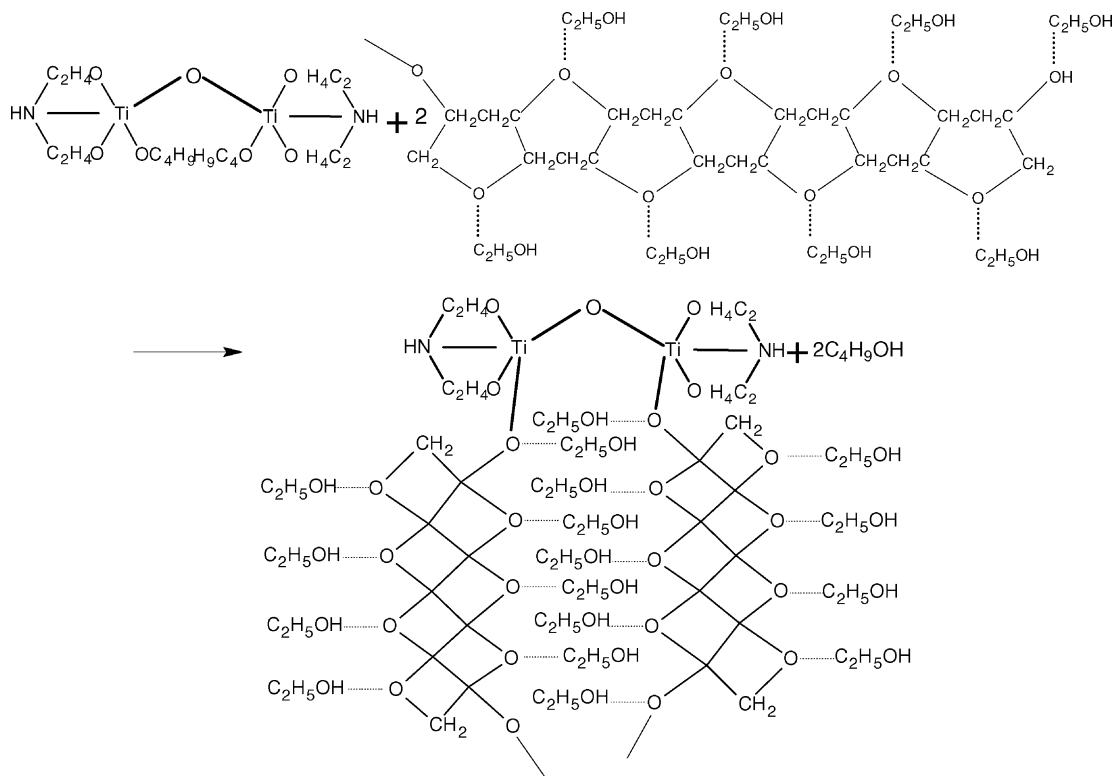
Fig. 2(a)–(c) shows SEM photographs of TiO_2 films with varied water/ $\text{Ti}(\text{OBU})_4$ molar ratios 1–3, respectively. It can be seen that the density of the pores decreased with the amount of water, while the pore size being the largest when water/ $\text{Ti}(\text{OBU})_4$ molar ratio was 2. This suggests that as the quantity of water is relatively low, the hydrolysis and polycondensation will run according to formulas (2a) and (3a), producing



which connects with PEG leading to the intermediate inorganic–organic network. After the removal of PEG upon thermal treatment, porous structure is retained in TiO_2 thin films. In the presented case, PEG plays a templating role in the formation of the inorganic porous structure.

3.2.2. Effect of complexing agents and solvents

Most of the proposed syntheses of porous titania rely on the control of the high reactivity of Ti(IV) towards hydrolysis and condensation, a problem of utmost importance. One suitable solution is the addition of complexing molecules as stabilizing agents. The aim of this procedure is to hinder the condensation reactions that lead to the rapid formation of



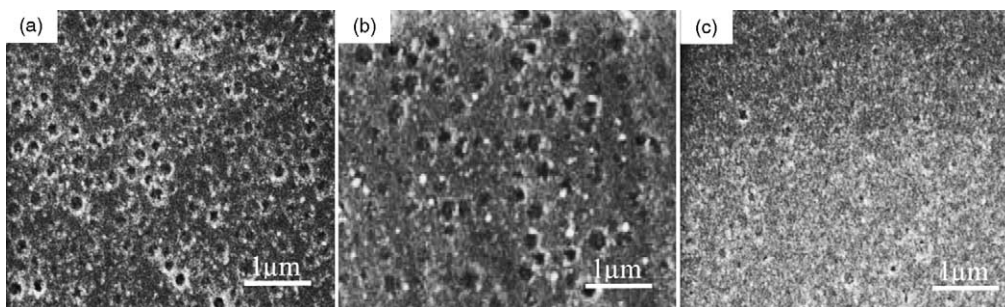


Fig. 2. SEM images of the surface morphology of TiO_2 films prepared from 0.5 g/100 ml PEG (2000) EtOH solution at water to $\text{Ti}(\text{OBu})_4$ ratio of (a) 1:1, (b) 2:1, and (c) 3:1.

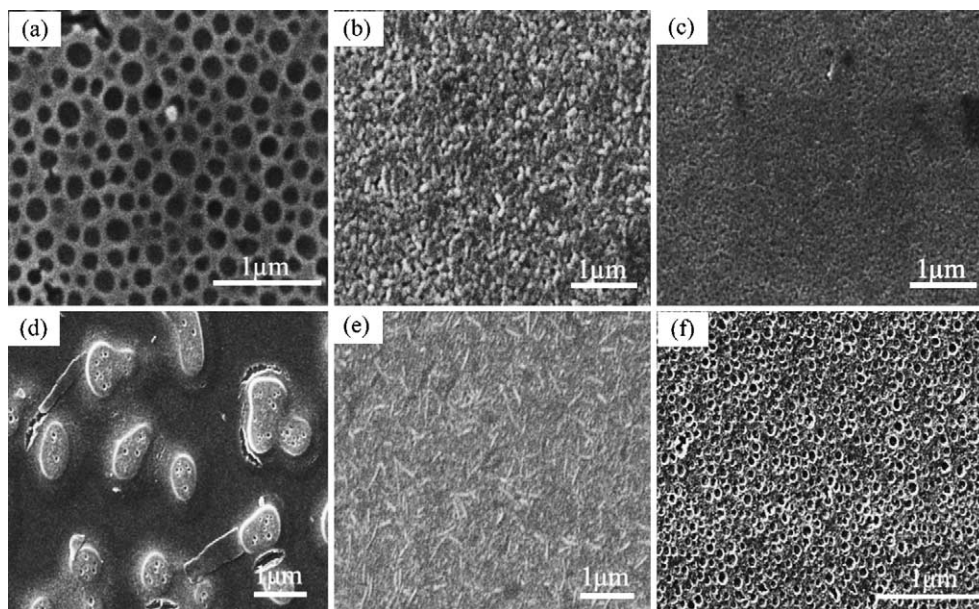
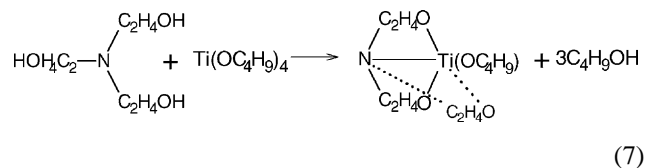
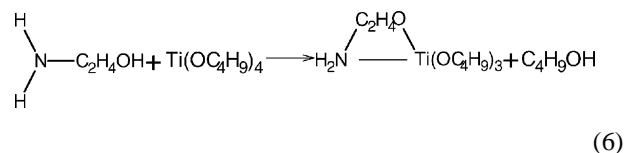


Fig. 3. SEM images of the surface morphology of TiO_2 films prepared from 4.0 g/100 ml PEG (1000) sol at water to $\text{Ti}(\text{OBu})_4$ ratio of 1:1 with complexing agents: (a) DEA, (b) TEA, (c) ACAC, (d) HAC, (e) H_3L , and solvents of (a) EtOH, and (f) *n*-butanol.


a dense inorganic network, yielding poorly textured material. So far, the effects of complex molecules on the structure of TiO_2 films have been rarely discussed. In our study, six different complexing agents were employed to compare their effects. Fig. 3 show SEM images of TiO_2 thin films made from the corresponding sol. Among the six complexing agents, the complexing ability of EA is not strong enough to inhibit the hydrolysis and condensation, inducing precipitate in the solution, so from which no TiO_2 coatings were obtained. The sample with DEA displays relatively regular pattern and periodic organization, the diameters of the pores being in the range 200–500 nm. While TEA, ACAC, and H_3L were used, the size and density of the pores decreased remarkably, the films with H_3L even had granular microstructure and flat texture. The addition of HAC caused phase separation in the precursor solution, as shown in Fig. 3(d), nevertheless, some pores could be observed on the “isolated islands”. FT-IR transmittance spectra for solutions containing different complexing agents (Fig. 4) provide

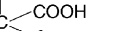
the evidence for the bonding of complexed groups to Ti ions. From trace 2 of Fig. 4, one can recognize that the absorption band appeared, which can be attributed to the absorption of N–Ti. And on the basis of the above analysis in Section 3.1, the interactions between EA/TEA and $\text{Ti}(\text{OBu})_4$ may be deduced to run following reactions (6) and (7), respectively.

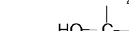


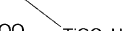
In the spectrum of trace 3, the appearance of C=O and O–Ti–O stretching vibration bands at 1583 and 1528 cm^{-1}


$$\text{Ti}(\text{OC}_4\text{H}_9)_4 + \text{C}_6\text{H}_6 \longrightarrow \text{C}_6\text{H}_5\text{Ti}(\text{OC}_4\text{H}_9)_3 + \text{C}_4\text{H}_9\text{OH} \quad (8)$$

(a) 

(b) 

(c) 

(d) 

(e) 

$$\begin{array}{c}
 \begin{array}{c} \text{CH}_2\text{COO} \\ | \\ \text{HO}-\text{C}-\text{COOH} \\ | \\ \text{CH}_2\text{COO} \end{array} \quad \begin{array}{c} \diagup \\ \diagdown \end{array} \quad \text{Ti}(\text{OC}_4\text{H}_9)_2 + \begin{array}{c} \text{Ti}(\text{OC}_4\text{H}_9)_2 \\ | \\ \text{O} \quad \text{COO} \\ | \quad | \\ \text{HOOCCH}_2-\text{C}-\text{CH}_2\text{COOH} \end{array} \rightleftharpoons (\text{OC}_4\text{H}_9)_2\text{Ti} \begin{array}{c} \diagup \quad \diagdown \\ \text{OOCCH}_2 \quad \text{HOOC} \\ | \quad | \\ \text{OOCCH}_2 \quad \text{C}-\text{O}-\text{C}(=\text{O})\text{CH}_2-\text{C} \begin{array}{c} \diagup \quad \diagdown \\ \text{O} \quad \text{COO} \\ | \quad | \\ \text{Ti}(\text{OC}_4\text{H}_9)_2 \end{array} \end{array} \text{CH}_2\text{COOH} + \text{H}_2\text{O}
 \end{array}$$
$$\text{CH}_3\text{COOH} + \text{Ti}(\text{OC}_4\text{H}_9)_4 \longrightarrow \text{CH}_3\overset{\text{O}}{\underset{\text{O}}{\parallel}}\text{C}-\text{O}-\text{Ti}(\text{OC}_4\text{H}_9)_3 + \text{C}_4\text{H}_9\text{OH} \quad (10)$$

The surface patterns of TiO₂ films prepared from solutions with EtOH and *n*-butanol as solvents, respectively, are presented in (a) and (f) of Fig. 3. It can be noted that the diameter of pores decreased greatly from 200–500 to 50–200 nm when EtOH is substituted with *n*-butanol, meanwhile the number of pores increasing obviously. This result can support our assumption in Section 3.1; the presence of *n*-butanol

$$\begin{array}{c} \text{C}_2\text{H}_4\text{O} \\ | \\ \text{HN} - \text{Ti} - \text{O} - \text{Ti} - \text{NH} \\ | \quad \quad | \quad \quad | \quad \quad | \\ \text{C}_2\text{H}_4\text{O} \quad \text{OC}_4\text{H}_9\text{C}_4\text{O} \quad \text{O} \quad \text{H}_4\text{C}_2 \\ | \quad \quad | \quad \quad | \quad \quad | \\ \text{C}_2\text{H}_4\text{O} \quad \text{OC}_4\text{H}_9\text{C}_4\text{O} \quad \text{O} \quad \text{H}_4\text{C}_2 \end{array}$$

3.3. Effect of PEG

The formation of porous structure in TiO_2 thin films strongly depends on the amount and type of PEG. SEM images for TiO_2 thin films prepared from the precursor solutions with different additions and molecular weights of PEG are shown in Fig. 5. It is observed that no pores appeared in TiO_2 films prepared from the solution without PEG. After PEG was added, different porous structures developed in the films. The size and density of the pores increased with increasing amount of PEG. The porous structure with

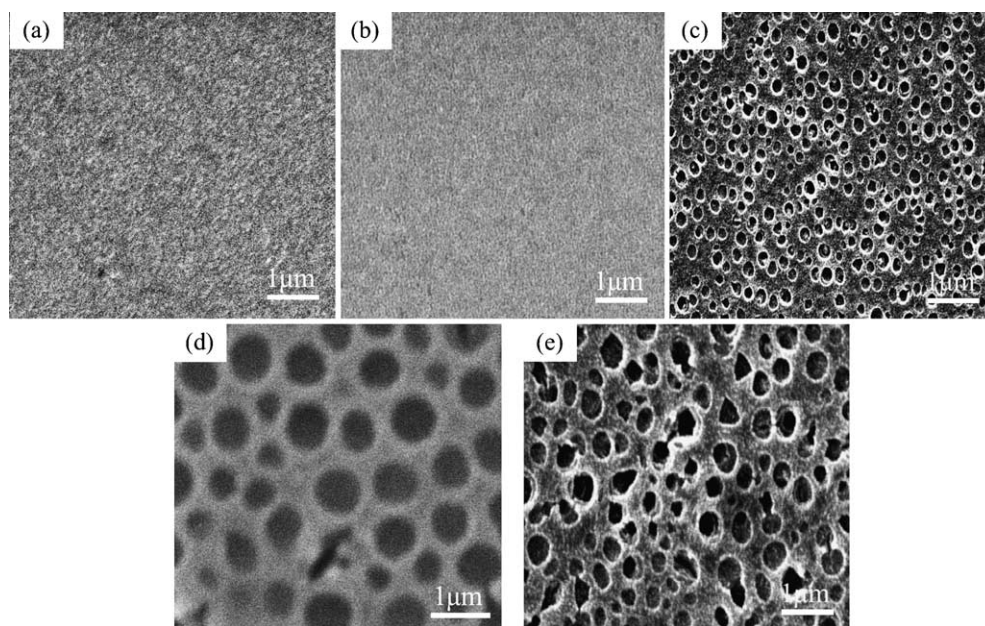


Fig. 5. SEM images of the surface morphology of TiO_2 films prepared from the precursor solution: (a) without PEG, (b) 1.0 g PEG (1000)/100 ml, (c) 2.0 g PEG (1000)/100 ml, (d) 4.0 g PEG (1000)/100 ml, and (e) 2.0 g PEG (2000)/100 ml.

a better arrangement is formed with increasing addition of the templates. The diameters of the pores in the films prepared from the solution containing 1.0, 2.0, and 4.0 g PEG (1000) were approximately 10, 50–100 and 200–500 nm, respectively.

The porous structure of TiO_2 thin films has been also found to be related to the molecular weight of PEG. SEM images (c) and (e) of Fig. 5 show that the pore size of the film sample with PEG (2000) was larger than that with PEG (1000), the density of pores being lower. It is supposed that the self-organization ability of PEG in sol is different for different molecular weights even at the same content. The PEG

dependence of the porous structure of TiO_2 films has been corroborated by N_2 adsorption measurement as presented in Fig. 6. It can be observed that BET surface area of TiO_2 films was enhanced with increasing PEG content and reached as high as 72 and $62 \text{ m}^2/\text{g}$, at 2.0 g/100 ml PEG (1000) and 1.0 g/100 ml of PEG (2000), respectively. However, it was decayed with a further increment of PEG content, which is due to the link-up of the pores and the reduction on pore number. As a result of the larger pore size and lower pore number, the surface area of TiO_2 films with PEG (2000) is smaller than that with PEG (1000).

4. Conclusions

TiO_2 porous thin films can be synthesized in such a sol–gel system using PEG as a template and $\text{Ti}(\text{OBU})_4$ as a precursor. The porous structure of TiO_2 thin films was found to significantly depend on the synthesis condition, such as the molar ratio of water to $\text{Ti}(\text{OBU})_4$, the species of complexing agents and solvents, specially the adding amount and molecular weight of PEG. The chemistry of the sol–gel progress is under discussion to provide directions tailoring the texture of porous TiO_2 films, aiming at a high degree of regularity and order of the porous structure with a large surface area.

Acknowledgements

The authors (Z.G. Jin, S.J. Bu) gratefully acknowledge financial support from Natural Science Foundation of Tianjin.

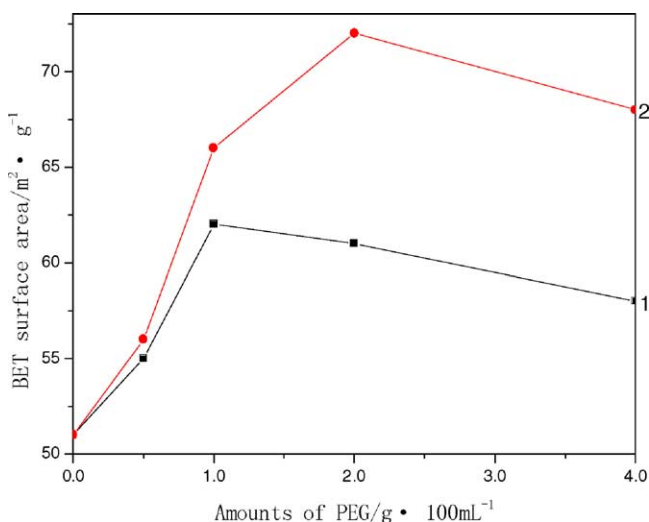


Fig. 6. BET surface area of TiO_2 films prepared from solution containing: (1) PEG (2000), (2) PEG (1000).

References

1. Fujishima, A. and Honda, K., Electrochemical photolysis of water at a semiconductor electrode. *Nature* 1972, **37**, 238–245.
2. Yu, J. C., Yu, J. G. and Zhao, J. C., Enhanced photocatalytic activity of mesoporous and ordinary TiO₂ thin films by sulfuric acid treatment. *Appl. Catal. B: Environ.* 2002, **36**, 31–43.
3. Gebeyehu, D., Brabec, C. J. and Sariciftci, N. S., Solid-state organic/inorganic hybrid solar cells based on conjugated polymers and dye-sensitized TiO₂ electrodes. *Thin Solid Films* 2002, **403/404**, 271–274.
4. Stamate, M.D., Dielectric properties of TiO₂ thin films deposited by a dc magnetron sputtering system. *Thin Solid Films* 2000, **372**, 246–249.
5. Dinh, N. N., Oanh, N. T. T., Long, P. D., Bernard, M. C. and Hugot-Le Goff, A., Electrochromic properties of TiO anatase thin films prepared by a dipping sol–gel method. *Thin Solid Films* 2003, **423**, 70–76.
6. Fretwell, R. and Douglas, P., An active, robust and transparent nanocrystalline anatase TiO₂ thin film-preparation, characterisation and the kinetics of photodegradation of model pollutants. *J. Photochem. Photobiol. A: Chem.* 2001, **143**, 229–240.
7. O'Regan, B. and Gratzel, M., A low-cost, high efficiency solar cells based on dye-sensitized colloidal TiO₂. *Nature* 1991, **353**, 737–739.
8. Grant, C. D., Schwartzberg, A. M., Smestad, G. P., Kowalik, J., Tolbert, L. M. and Zhang, J. Z., Characterization of nanocrystalline and thin film TiO₂ solar cells with poly(3-undecyl-2,2'-bithiophene) as a sensitizer and hole conductor. *J. Electroanal. Chem.* 2002, **522**, 40–48.
9. Yun, H. S., Miyazawa, K. C., Honma, I., Zhou, H. S. and Kuwabara, M., Synthesis of semicrystallized mesoporous TiO₂ thin films using triblock copolymer templates. *Mater. Sci. Eng.* 2003, **23**, 487–494.
10. Shimizu, K., Imai, H., Hirashima, H. and Tsukuma, K., Low-temperature synthesis of anatase thin films on glass and organic substrates by direct deposition from aqueous solutions. *Thin Solid Films* 1999, **351**, 220–224.
11. Teresa Viseu, M. R. and Ferreira, M. I. C., Morphological characterization of TiO₂ thin films. *Vacuum* 1999, **52**, 115–120.
12. Blesic, M. D., Saponjic, Z. V., Nedeljkovic, J. M. and Uskokovic, D. P., TiO₂ films prepared by ultrasonic spray pyrolysis of nanosize precursor. *Mater. Lett.* 2002, **54**, 298–302.
13. Zhang, D. S., Yoshida, T. and Minoura, H., Low-temperature fabrication of efficient porous titania photoelectrodes by hydrothermal crystallization at the solid/gas interface. *Adv. Mater.* 2003, **15**(10), 814–817.
14. Mills, A., Elliott, N., Parkin, I. P., O'Neill, S. A. and Clark, R. J., Novel TiO₂ CVD films for semiconductor photocatalysis. *J. Photochem. Photobiol. A: Chem.* 2002, **151**, 171–179.
15. Zhu, Y. C. and Ding, C. X., Plasma spraying of porous nanostructured TiO₂ film. *NanoStruct. Mater.* 1999, **11**, 319–323.
16. Iwata, T., Ishikawa, M., Ichino, R. and Okido, M., Photocatalytic reduction of Cr(VI) on TiO₂ film formed by anodizing. *Surf. Coat. Technol.* 2003, **169/170**, 703–706.
17. Ting, C. C., Chen, S. Y. and Liu, D. M., Preferential growth of thin rutile TiO₂ films upon thermal oxidation of sputtered Ti films. *Thin Solid Films* 2002, **402**, 290–295.
18. Ichinose, H., Terasaki, M. and Katsuki, H., Preparation of a nanocrystalline titanium dioxide negative electrode for the rechargeable lithium ion battery. *J. Ceram. Soc. Jpn.* 1996, **104**, 715–718.
19. Buscema, C. L., Malibert, C. and Bach, S., Elaboration and characterization of thin films of TiO₂ prepared by sol–gel process. *Thin Solid Films* 2002, **418**, 79–84.
20. Baythoun, M. S. G. and Sale, F. R., Production of strontium-substituted lanthanum manganite perovskite powder by the amorphous citrate process. *J. Mater. Sci.* 1982, **17**, 2757–2769.